Rev. Roum. Sci. Techn.– Électrotechn. et Énerg.
Vol. **69**, *1*, pp. 39–44, Bucarest, 2024

SECOND ORDER SLIDING MODE CONTROL FOR ISLANDED AC MICROGRIDS WITH RENEWABLE POWER RESOURCES

NAVID REZA ABJADI[1*], ABBAS KARGAR[1]

Keywords: Microgrid (MG); Master-slave strategy; Power control; Second order sliding mode control; Voltage control.

Microgrids have attracted much attention and are the future of power systems. This paper proposes a new control scheme for islanded ac microgrid (MG) using the master-slave technique. Stability and high performance are vital for islanded MG. Two second-order sliding mode controls (SMCs) are designed in stationary reference frames for master and slave units to control voltage and power. Both designed controls guarantee the convergence of considered outputs to their reference values. The proposed controls are robust, simple, and chattering-free, and only require local measurements. The control method proposed in this paper can be easily extended to microgrids with any number of slave units and parallel connected inverters. The effectiveness of the proposed control scheme is verified through simulation results in MATLAB/Simulink environment and compared to feedback linearization control and a modified conventional SMC.

1. **INTRODUCTION**

Climate change and environmental pollution caused by fossil fuels cannot be ignored. Green energy sources can be used to overcome these problems. Distributed generation (DG) sources such as wind turbines and photovoltaic systems will play an important role in future power systems. The increasing penetration of DGs needs new approaches and solutions to improve designs and electricity utilization. Most DG sources are interfaced to the network through a voltage source inverter (VSI).

An MG is a group of connected power sources and loads [1]. MGs can provide grid demand, improve power quality, and guarantee electrical continuity to local loads in grid faults [2]. In [1], a grid-connected MG is investigated, and a control scheme is proposed under unbalanced conditions. MG can be employed by DG sources where power transmission is far away or the MG is disconnected from the main grid because of a fault. In this case, the MG is called islanded MG [3]. In [4], a voltage and frequency control approach is proposed for DGs in islanded MG based on proportional-integral (PI) control. In [5], two additional control signals are generated to improve the stability of an MG by applying a small signal approach. Both proposed control schemes of [4,5] suffer from large overshoots and oscillations considering large disturbances.

Different strategies fall into two main categories: to control the DGs and to share the power between DGs in an isolated MG, which are communication-free and communication-based strategies [6,7]. Droop control is a communication-free strategy that only needs local information [8]; however, it doesn't have a fast response, and it may cause some stability problems. A medium voltage MG is studied in [9,10], and employing a droop control strategy, the control and power sharing between DGs are achieved under balanced and unbalanced conditions. Dc bus voltage deviation is also a main disadvantage of the conventional droop control [11]. The main communication-based strategies are centralized control, distributed control, and master-slave (MS) strategy. Centralized control needs all the information, and with a small failure, the whole system crashes. Distributed control and MS strategy need less MG information, so a low bandwidth link is necessary. MS strategy can result in very good power sharing and can be implemented easily [6,7].

In the MS strategy, the largest DG, the master unit (MU), is considered, and the other DGs are the slave units (SU). The MU controls the voltage and frequency, while each SU controls its generated active and reactive powers [6]. It can be shown that the MS strategy can be used well in parallel inverters, and it can also be used in islanded multi-bus ac MGs; however, the performance is degraded when the magnitudes of the line impedances are high since the voltages of the SUs are not controlled directly. In [2], some power-sharing issues of MS strategy are addressed, and the communication needed in MS control is discussed. In [12], a two-level control strategy for MS control MG is introduced, which does not have a good dynamic response and isn't robust against uncertainties and disturbances.

In [6], adopting the MS strategy using PI control, the effect of communication delay in a simple MG, which included two parallel inverters, is investigated. The PI control tuning depends on the operating point of the DGs.

A communication-free master-slave MG is presented in [3]. In [13], μ-synthesis is used for MG MS control. The problem is that μ-synthesis using DK iteration is usually high order, and a sophisticated design with large matrices is needed. In [14], the influence of coefficients of conventional decoupling controls with PI controllers in MS control is investigated using small signal quantities. In [15], a cascaded PI-based voltage and current control using the MS strategy in islanded MG is investigated.

Conventional sliding mode control (SMC) is a robust nonlinear control technique commonly using a discontinuous term in control law to achieve high-performance behavior despite uncertainties. SMC can be implemented easily and can be used for trajectory tracking problems. In [16], an adaptive SMC is designed to control the voltage of the bus connected to the MU, and an adaptive feedback linearization (FBL) control is designed to control each SU's active and reactive powers. The proposed adaptive SMC of [16] estimates the bounds of lumped uncertainties. There is no guarantee that the estimated bounds converge to their real values. Large, estimated bounds, multiplied by the sign or saturation functions, result in high control effort and much chattering. In addition, lumped uncertainties are also considered in the designed adaptive FBL control [16]. Again, large estimated lumped uncertainties cause high control effort.

High-order SMCs are robust controls that can eliminate the chattering effect [17]. In [18], the implementation of two second-order SMCs for a buck converter is investigated, and it

[1] Faculty of Engineering, Shahrekord University, Shahrekord, Iran
E-mails: abjadi.navidreza@sku.ac.ir (*corresponding author), kargar@sku.ac.ir

DOI: 10.59277/RRST-EE.2024.69.1.7

is shown that the chattering effect is quite reduced and a high-performance control response is obtained. In [19], some high-order SMCs are designed for an MG adopting a centralized control scheme that is very complicated and must be redesigned if the loads or the DGs change.

The super-twisting algorithm (STA) is a continuous 2nd-order SMC without chattering phenomena that can be used to achieve a robust control [20]. STA is suitable for perturbed systems with relative degree one [21]. The algorithm with the prescribed law of variation (PLV) is another continuous 2nd-order SMC suitable for systems with relative degree two [17].

This paper focuses on the control of DGs of an islanded MG using the MS strategy. Two types of 2nd-order SMCs are designed for master and slave units. PLV control is designed to control the bus voltage connected to MU, and STA control controls the active and reactive powers delivered by SUs. There is a symmetry in control design since, for both master and slave units, 2nd-order SMCs are used. The novelty and contributions of the paper are designing two different 2nd-order SMCs, one for MU and the other for Sus, with perfect tracking, robustness, and chattering-free properties despite the simple structure of the controls. The paper's organization is as follows: section 2 represents the state-space model of the DGs and their appropriate controls. In section 3, simulation results are presented and discussed. Finally, section 4 states the main conclusions of the paper.

2. DGS MODELING AND CONTROL

A DG unit including VSI and LC filter is shown in Fig. 1. Applying Kirchhoff's voltage and current laws in the stationary reference frame, one can obtain

$$\mathrm{d}\mathbf{i}_f/\mathrm{d}t = a(\mathbf{v}_i - b\mathbf{i}_f - \mathbf{v}_f), \quad (1)$$

$$\mathrm{d}\boldsymbol{v}_f/\mathrm{d}t = c(\boldsymbol{i}_f - \boldsymbol{i}_o), \quad (2)$$

where $\mathbf{i}_f = [i_{f\alpha}\, i_{f\beta}]^T$, $\mathbf{v}_i = [v_{i\alpha}\, v_{i\beta}]^T$, $\mathbf{v}_f = [v_{f\alpha}\, v_{f\beta}]^T$, $a = 1/L_f$, $b = R_f$ and $c = 1/C_f$.

The active and reactive powers injected into the filter bus are given by [14]

$$P = 1.5(v_{f\alpha}i_{f\alpha} + v_{f\beta}i_{f\beta}), \quad (3)$$

$$Q = 1.5(v_{f\beta}i_{f\alpha} - v_{f\alpha}i_{f\beta}). \quad (4)$$

Because of the robustness, chattering free property, and simplicity of 2nd-order SM controllers; two versions of these controllers are designed for master and slave units. Besides, feedback linearization control and a modified conventional SMC are also presented.

The n^{th}-order SM is determined by $s = \dot{s} = \ddot{s} = s^{(n-1)}$, where s is the sliding variable [17].

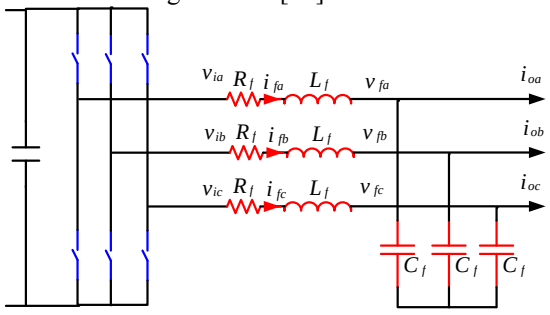

Fig. 1 – A DG unit including VSI and LC filter.

Figure 2 illustrates the phase trajectories of two 2nd-order SMCs: the super twisting algorithm and the prescribed law of variation [17]. The trajectories achieve origin smoothly in both controls.

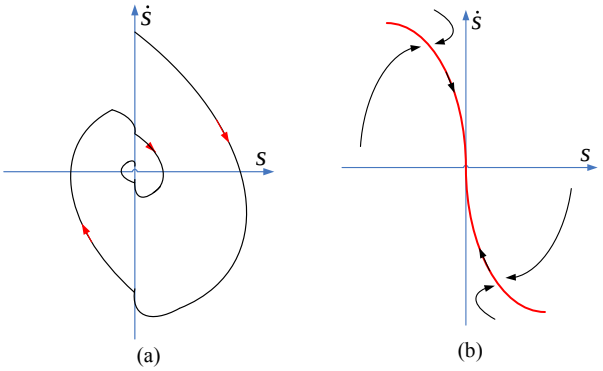

Fig. 2 – Phase trajectories of two 2nd-order SMCs named: a) super twisting algorithm; b) prescribe law of variation [17].

2.1. MU 2ND-ORDER SMC DESIGN

Consider the following vector, including sliding variables

$$\mathbf{S} = \mathbf{v}_f - \mathbf{v}_f^*, \quad (5)$$

where $\mathbf{S} = [S_\alpha\, S_\beta]^T$ and $\mathbf{v}_f^*$ is the voltage reference vector.

Differentiating $\mathbf{S}$ twice for time and substituting from (1) and (2),

$$\ddot{\mathbf{S}} = \ddot{\mathbf{v}}_f - \ddot{\mathbf{v}}_f^* = \mathrm{c}(\mathrm{d}\mathbf{i}_f/\mathrm{d}t - \mathrm{d}\mathbf{i}_o/\mathrm{d}t) - \ddot{\mathbf{v}}_f^* = ca\left(\mathbf{v}_i - b\mathbf{i}_f - \mathbf{v}_f\right) - c\mathrm{d}\mathbf{i}_o/\mathrm{d}t - \ddot{\mathbf{v}}_f^*. \quad (6)$$

In (6), $\boldsymbol{v}_i$ is the control input and the relative degree is 2; therefore, a PLV SMC can be designed.

Considering nominal parameters and equating $\ddot{\mathbf{S}}$ from (6) to 0, the equivalent control law is obtained as

$$\mathbf{v}_{ieq} = \bar{b}\mathbf{i}_f + \mathbf{v}_f + (\bar{c}\mathrm{d}\mathbf{i}_o/\mathrm{d}t + \ddot{\mathbf{v}}_f^*)/(\bar{c}\bar{a}) \quad (7)$$

where $\bar{a}$, $\bar{b}$ and $\bar{c}$ are the nominal values of a, b and c respectively. The reaching control law based on the PLV method is given by [19]

$$\mathbf{v}_{ireach} = -V_M \mathrm{sgn}(\dot{\mathbf{S}} + \gamma|\mathbf{S}|^{\frac{1}{2}}\mathrm{sgn}(\mathbf{S})), \quad (8)$$

where V_M and γ are positive constants.

The control law is given by

$$\mathbf{v}_i = \mathbf{v}_{ieq} + \mathbf{v}_{ireach}. \quad (9)$$

It is worthwhile to note that if $\mathbf{v}_i$ is chosen as follows, an FBL control or a modified conventional SMC is obtained

$$\mathbf{v}_i = \mathbf{v}_{ieq} - K_1\dot{\mathbf{S}} - K_2\mathbf{S}, \quad (10)$$

$$\mathbf{v}_i = \mathbf{v}_{ieq} - K_1\mathrm{sgn}(\mathbf{S}) - K_2\mathbf{S}, \quad (11)$$

where K_1 and K_2 are positive constants.

2.2. SU 2ND-ORDER SMC DESIGN

Differentiating active and reactive powers from (3) and (4) concerning time and substituting from (1) and (2), one can obtain

$$\dot{P} = f_P + u_P, \quad (12)$$

$$\dot{Q} = f_Q + u_Q, \quad (13)$$

where

$$f_P = 1.5c\left[(i_{f\alpha} - i_{o\alpha})i_{f\alpha} + (i_{f\beta} - i_{o\beta})i_{f\beta}\right] - -1.5a[(bi_{f\alpha} + v_{f\alpha})v_{f\alpha} + (bi_{f\beta} + v_{f\beta})v_{f\beta}], \quad (14)$$

$$u_P = 1.5a(v_{f\alpha}v_{i\alpha} + v_{f\beta}v_{i\beta}), \quad (15)$$

$$f_Q = 1.5c\left[(i_{f\beta} - i_{o\beta})i_{f\alpha} - (i_{f\alpha} - i_{o\alpha})i_{f\beta}\right] - -1.5a[(bi_{f\alpha} + v_{f\alpha})v_{f\beta} - (bi_{f\beta} + v_{f\beta})v_{f\alpha}], \quad (16)$$

$$u_Q = 1.5a(v_{f\beta}v_{i\alpha} - v_{f\alpha}v_{i\beta}). \quad (17)$$

Consider the following sliding variables

$$S_P = P - P^*, \quad (18)$$

$$S_Q = Q - Q^*. \quad (19)$$

Differentiating (18) and (19) concerning time and substituting from (12) and (13), one can obtain

$$\dot{S}_P = f_P + u_P, \quad (20)$$

$$\dot{S}_Q = f_Q + u_Q. \quad (21)$$

In (20) and (21), u_P and u_Q are the control inputs, and the relative degrees are 1; therefore, an STA SMC can be designed. Considering nominal parameters and equating $\dot{S}_P$ and $\dot{S}_Q$, the equivalent control laws are obtained as

$$u_{Peq} = -\bar{f}_P, \quad (22)$$

$$u_{Qeq} = -\bar{f}_Q, \quad (23)$$

where $\bar{f}_P$ and $\bar{f}_Q$ are the nominal values of f_P and f_Q respectively.

The reaching control law based on the STA method is given by [19]

$$u_{ireach} = -K_3 \int \text{sgn}(S_i)\, dt - K_4 |S|^{\delta} \text{sgn}(S), \quad (24)$$

where $i \in \{P, Q\}$; K_3 and K_4 are positive constants and $0 < \delta < 1$. The control law is given by

$$u_i = u_{ieq} + u_{ireach}. \quad (25)$$

It is worthwhile to note that if u_i is chosen as follows, an FBL control or a modified conventional SMC is obtained

$$u_i = u_{ieq} - K_4 S_i, \quad (26)$$

$$u_i = u_{ieq} - K_3 \text{sgn}(S_i) - K_4 S_i. \quad (27)$$

3. SIMULATION RESULTS

To investigate the validity of the designed 2nd-order SMCs for the islanded MGs, the MG of [9,10,16] is simulated in MATLAB/SImulink which is presented in Fig. 3.

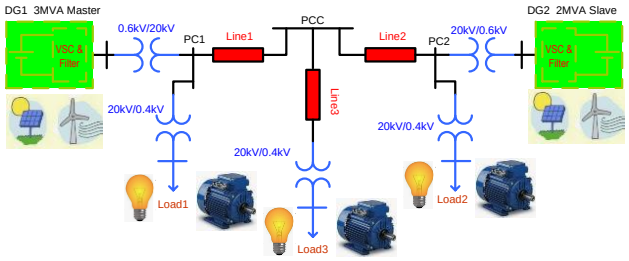

Fig. 3 – A MG with two DGs.

This case represents the normal testing conditions for the proposed controls. Only the MU provides the powers from t = 0 s to t = 0.1 s. From t = 0.1s to t = 0.15 s the active and reactive powers of SU change from 0 to 0.2 pu and 0.1 pu linearly, respectively.

DG1 and DG2 are considered as MU and SU respectively. For simplicity such an MG is studied; nevertheless, the models and controls can be used for MGs with any number of DGs. Figure 4 shows the Simulink block diagram. The solver is the fixed-step type with a discrete sample time of 5μs. The fixed-step discrete solver with a suitable sample time results in a fast and accurate simulation. The parameters of the MG are given in Table 1.

Table 1

The parameters of the MG

The nominal (base) power	3 MVA
VSIs line to line nominal voltage	600 V
MG frequency	50 Hz
VSIs filter resistance	0.002 Ω
VSIs filter inductance	500 μH
VSIs filter capacitance	400 μF
VSIs DC bus voltage	1500 V
VSIs Switching frequency	2 kHz
Line1 impedance	0.35+j 0.785 Ω

The master DG nominal power and the VSIs line-to-line nominal voltage are base values. The MG is tested and examined under four different cases. The parameters of the controllers are given in Table 2.

Table 2

The parameters of the controllers

The proposed control scheme	V_M=500, γ=1e4, δ=0.5 K_3=1e5,K_4=1e4
FBL control	K_1=50,K_2=500,K_4=1e5
Conventional SMC	K_1=20,K_2=300,K_3=15,K_4=1e5

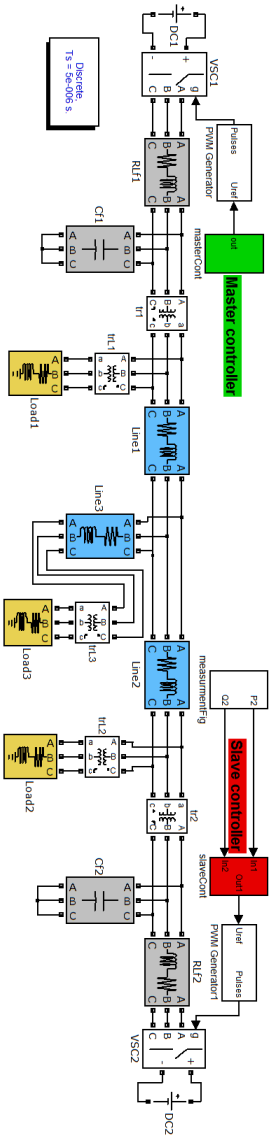

Fig. 4 – The SIMULINK block diagram.

3.1. CASE 1

The simulation results, including the voltage, active and reactive powers of three buses (PC1, PC2, and Load3), are shown in Fig. 5. It is seen that the powers track their references perfectly. As the SU powers increase, the MU powers decrease. The voltages are sinusoidal, and the MU bus amplitude and frequency are controlled properly. At t = 0.3 s, the active and reactive powers of SU change to zero, and the MU provides all the demand power. No voltage deviation is observed, and the dynamic responses are acceptable without low-frequency oscillations. The voltage THDs at different buses are below the 2.5 % required by IEEE 1547 and IEC 61727 standards (50 % of the current harmonic limits) [22].

3.2. CASE 2

In this case, all the testing conditions are similar to the ones described in case 1; however, the controllers are FBL

controllers. The simulation results are shown in Fig. 6. Compared to case 1, there are some oscillations in the active and reactive powers of MU and Load3, which are the results of the visible increase and decrease in voltages. Using FBL control, the MU voltage tracking could be better than the tracking in case 1. In addition, FBL control is not robust enough to control parameter uncertainties and disturbances.

3.3. CASE 3

Again, all the testing conditions are like the ones described in case 1; however, the controllers are modified conventional SM controllers. The simulation results are shown in Fig. 7. The effect of chattering is very evident. The voltages and powers are affected seriously and include high-frequency content. VSI filters cannot clear these high-frequency contents. It is worthwhile to note that chattering phenomena can also excite unmodeled modes and cause instability in the practical real system; moreover, it increases the power loss of VSI.

The performance of case 1 (proposed control scheme), case 2 (FBL control), and case 3 (conventional SMC) can be compared based on various factors and indices, such as their ability to track the reference accurately. In Table 3, the integral absolute error (IAE) of α-axis voltage and β-axis voltage for the PC1 bus and active and reactive powers for the PC2 bus are represented.

Table 3

The IAE indices for cases 1 to 3

index / control	IAE of α-axis voltage	IAE of β-axis voltage	IAE of P	IAE of Q
Proposed control scheme	7.05	6.5	1333	1189
FBL conrol	25.5	31	1165	1065
Conventional SMC	37.8	38.6	49170	28600

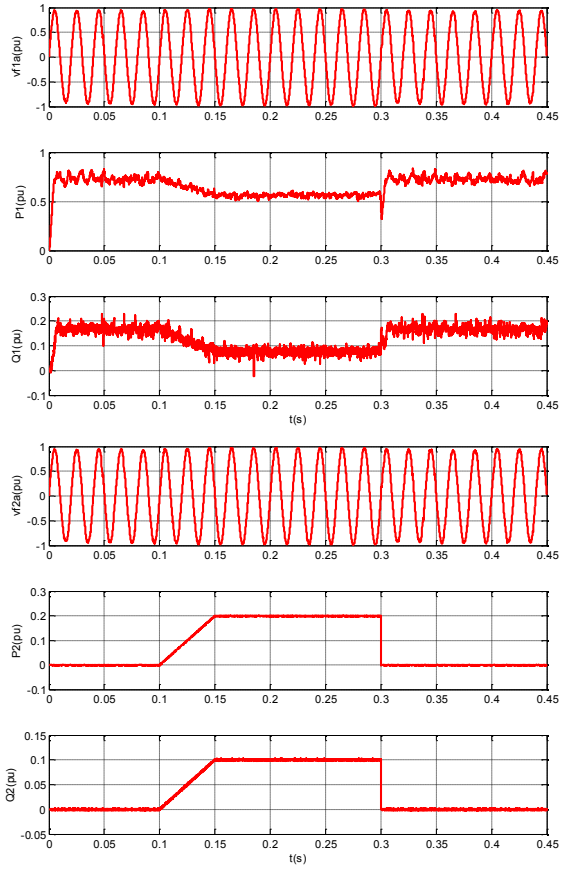

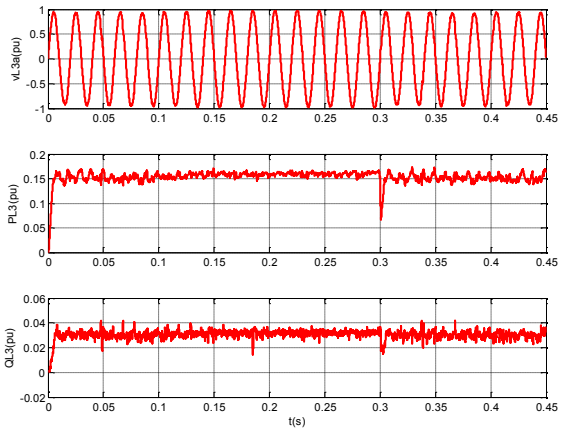

Fig. 5 – Case 1. Proposed control scheme: voltage, active and reactive power of three buses.

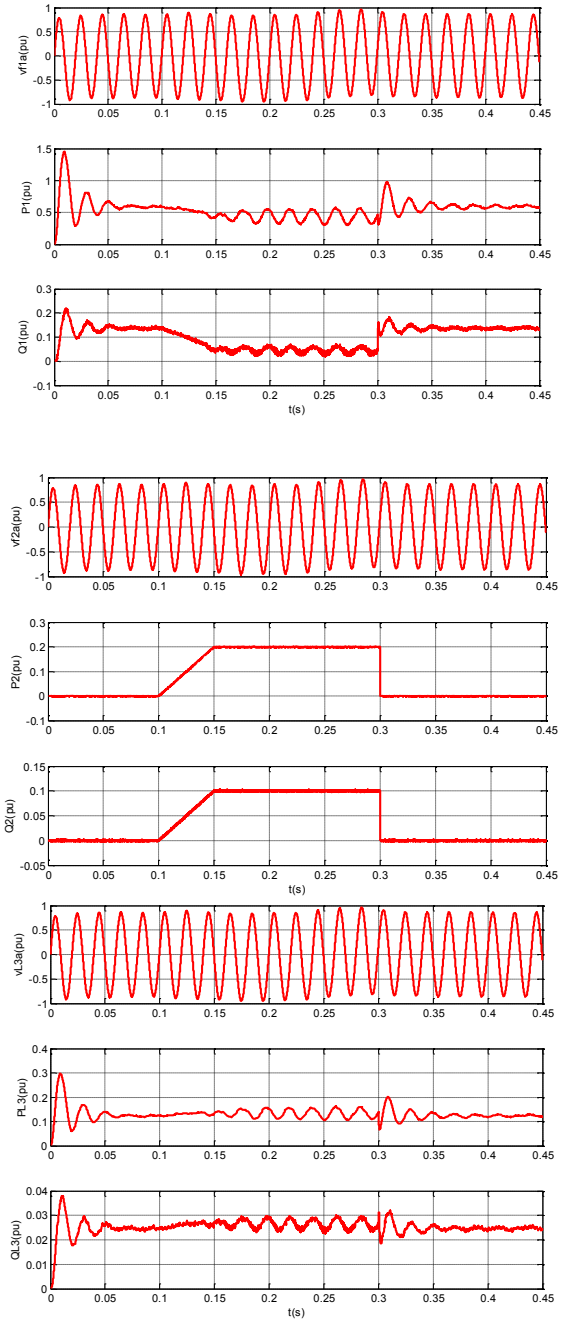

Fig. 6 – Case 2. FBL control: voltage, active, and reactive power of three buses.

3.4. CASE 4

This case is like case 1; however, a nonlinear load (rectifier) is paralleled to Load 3 at time 0.25 s. The simulation results are shown in Fig. 8. The increasing penetration of loads with power electronics converters increases harmonic distortions in the MGs due to the inherent nonlinear nature of power electronics switches. Using the proposed controls, it is seen that despite the harmonics in Line 3 current, the voltages remain sinusoidal, and the required powers are provided by MU and SU properly. Using the proposed controls, the MG operates smoothly and is acceptable. The effect of harmonic load on voltages and powers is negligible. This case illustrates the robustness of the proposed SMCs.

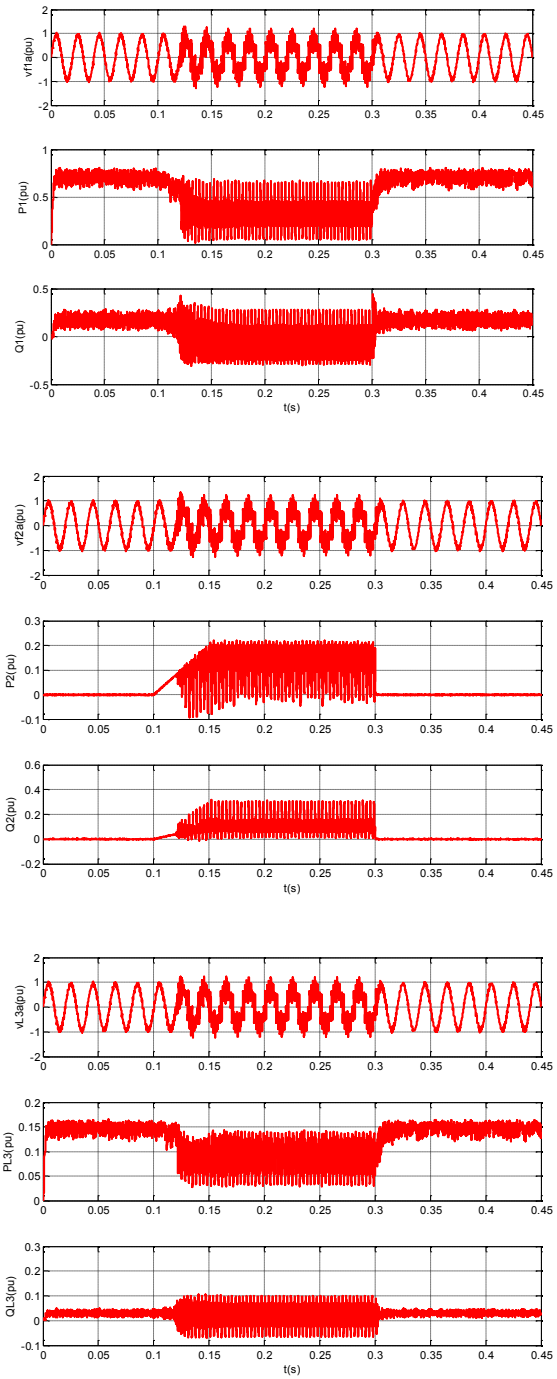

Fig. 7 – Case 3. Conventional SMC: voltage, active, and reactive power of three buses.

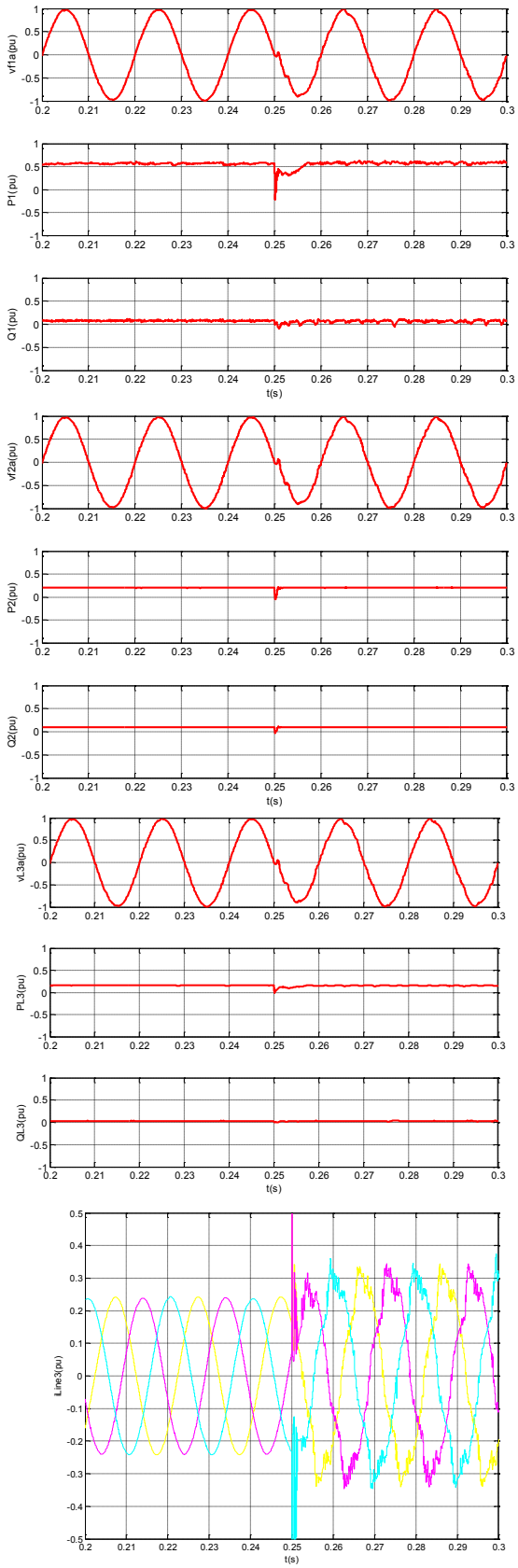

Fig. 8 – Case 4. Proposed control scheme with harmonic load (rectifier): voltage, active and reactive power of three buses.

3.4. DISCUSSION

Thanks to the decoupling between voltage control and active/reactive powers control in MS strategy, these variables can be controlled easily. The obtained results illustrate the superiority of the proposed control scheme's steady state and

dynamic performance in all considered conditions regarding reference voltage tracking for MU and active or reactive powers increase or decrease for SU.

The stability and tracking performance of the voltage and active/reactive power control is improved significantly using the proposed control scheme. The IEA indices in Table 3 prove the improvement in reducing the tracking errors.

It is worth noting the parameters of the different controllers are tuned by trial-and-error method to obtain the best desired outcomes, and when the range of these parameters are obtained, the control system is not very sensitive to small changes of them. The proposed control scheme is well-designed and has more parameters, which results in the best performance. The conventional SMC suffers from chattering phenomena, which causes instability in some circumstances.

4. **CONCLUSIONS**

MG is an exciting system that delivers electrical power to local loads. In this paper, two 2nd-order SMCs are designed for islanded MGs with inverter-based DGs. MS strategy controls MG's voltage amplitude, frequency, and injected powers. Simulation results are presented for an MG with two DGs without dropping generality. Three controllers (2nd-order SM, FBL, and modified conventional SM controllers) are compared for each MU and SU. The obtained results show the superiorities of the proposed 2nd-order SMCs. The voltage of the MU bus and the injected powers of the SU are controlled perfectly. By changing the loads or the power references of the SU, the MU meets the remaining load demand, and good load sharing between VSIs is achieved. Using the proposed control scheme, no significant overvoltage or undervoltage is observed during the transients, and a good and reliable control is obtained. In addition, the volatility inherent to the DGs is addressed properly, and the DGs can inject their power when available. The main advantages of the proposed control scheme are the simple structure of controllers, perfect tracking, robustness, and chattering-free properties of controllers. The designed 2nd-order SMCs can control the voltage and the powers of any VSI. It is worth mentioning here that to employ the proposed control scheme in a real MG, a secondary control is needed, which provides references. Also, special considerations are needed for accurate calculations to implement the fractional orders in control terms. Finally, for future research, renewable energy resources such as photovoltaic or wind can be considered in the MG, and the proposed control scheme is investigated with the corresponding MPPT algorithms.

ACKNOWLEDGMENTS

This research is supported by the Design of Photovoltaic Systems Research Core, Shahrekord University.

Received on 19 April 2023

REFERENCES

1. M.M. Rezaei, J. Soltani, *A robust control strategy for a grid-connected multi-bus microgrid under unbalanced load conditions*, International Journal of Electrical Powers, and Energy Systems, **71**, pp. 68–76 (2015).
2. T. Caldognetto, P. Tenti, *Microgrids operation based on master-slave cooperative control*, IEEE Journal of Emerging and Selected Topics in Power Electronics, **2**, *4*, pp. 1081–1088 (2014).
3. P. Monshizadeh, C. De Persis, N. Monshizadeh. A. van der Schaft, *A communication-free master-slave microgrid with power sharing*, 2016 American Control Conference (ACC), Boston, USA, 2016.
4. P. Kumar, M. Kumar, N. Pal, *An efficient control approach of voltage and frequency regulation in an autonomous microgrid*, Rev. Roum. Sci. Techn. – Électrotechn. et Énerg., **66**, *1*, pp. 33–39 (2021).
5. Y. Daili, A. Harrag, *Improved decoupling virtual synchronous generator control strategy*, Rev. Roum. Sci. Techn. – Électrotechn. et Énerg., **66**, *3*, pp. 153–160 (2021).
6. A. Alfergani, A. Khalil, *Modeling and control of master-slave microgrid with communication delay*, The 8th International Renewable Energy Congress (IREC 2017), 2017.
7. H. Han, X. Hou, J. Yang, J. Wu, M. Su, J.M. Guerrero, *Review of power-sharing control strategies for islanding operation of ac microgrids*, IEEE Trans. On Smart Grid, **7**, *1*, pp. 1–16 (2015).
8. J. Pinto, A. Carvalho, V. Morais, *Power sharing in island microgrids*, Frontiers in Energy Research, **8**, Article 609218, pp. 1–14 (2021).
9. A. Ghazanfari, M. Hamzeh, H. Mokhtari, H. Karimi, *Active power management of multihybrid fuel cell/supercapacitor power conversion system in a medium voltage microgrid*, IEEE Trans. on Smart Grid, **3**, *4*, pp. 1903–1910 (2012).
10. M. Hamzeh, H. Karimi, H. Mokhtari, *A new control strategy for a multi-bus mv microgrid under unbalanced conditions*, IEEE Trans. on Power Systems, **27**, *4*, pp. 2225–2232 (2012).
11. P.J. dos Santos Neto, T.A.S. Barros, J.P.C. Silveira, E.R. Filho, J.C. Vasquez, J.M. Guerrero, *Power management techniques for grid-connected dc microgrids: a comparative evaluation*, Applied Energy, **269**, 115057, pp. 1–15 (2020).
12. M.S. Mahmoud, O. Al-Buraiki, *Two-level control for improving the performance of microgrid in islanded mode*, 2014 IEEE 23rd International Symposium on Industrial Electronics (ISIE), Istanbul, Turkey, pp. 54–59 (2014).
13. T. Yao, R. Ayyanar, *Variable structure robust voltage regulator design for microgrid master-slave control*, 2017 IEEE Energy Conversion Congress and Exposition (ECCE), Cincinnati, OH, USA, 2017).
14. H. Liang, Y. Dong, Y. Huang, C. Zheng, P. Li, *Modeling of multiple master–slave control under island microgrid and stability analysis based on control parameter configuration*, Energies, **11**, 2223, pp. 1–18 (2018).
15. J. Marchgraber, W. Gawlik, *Investigation of black-starting and islanding capabilities of a battery energy storage system supplying a microgrid consisting of wind turbines, impedance- and motor-loads*, Energies, **13**, 5170, pp. 1–24 (2020).
16. M.M. Rezaei, J. Soltani, *Robust control of an islanded multi-bus microgrid based on input–output feedback linearization and sliding mode control*, IET Generation, Transmission & Distribution, **9**, *15*, pp. 2447–2454 (2015).
17. W. Perruquetti, J.P. Barbot, *Sliding mode control in engineering*, Marcel Dekker, Inc., NY, 2002.
18. A. Mehta, B. Naik, *Sliding mode controllers for power electronic converters*, Springer Nature, Singapore Pte Ltd., 2019.
19. M. Cucuzzella, G.P. Incremona, A. Ferrara, *Design of robust higher order sliding mode control for microgrids*, IEEE Journal on Emerging and Selected Topics in Circuits and Systems, **5**, *3*, pp. 393–401 (2015).
20. R. Seeber, M. Reichhartinger, *Conditioned super-twisting algorithm for systems with saturated control action*, Automatica, **116**, pp. 1–9 (2020).
21. H. Obeid, S. Laghrouche, L. Fridman, *A barrier function based-adaptive super-twisting controller for wind energy conversion system*, 2019 IEEE 58th Conference on Decision and Control (CDC), Palais des Congrès et des Expositions Nice Acropolis, Nice, France, December 11–13, pp. 7869–7874 (2019).
22. R. Teodorescu, M. Liserre, P. Rodriguez, *Grid converters for photovoltaic and wind power systems*, John Wiley & Sons, Ltd United Kingdom, 2011.